euspen's 24th International Conference & Exhibition, Dublin, IE, June 2024
www.euspen.eu

Precision plunge grinding with coarse-grained diamond grinding wheel

Barnabás Adam[1,2], Oltmann Riemer[1,2], Kai Rickens[1], Carsten Heinzel[1,2]

[1]*Leibniz Institut für Werkstofforientierte Technologien IWT, Laboratory for Precision Machining LFM, Badgasteiner Straße 2, 28359 Bremen, Germany*
[2]*MAPEX Center for Materials and Processes, University of Bremen, Germany)*

adam@iwt.uni-bremen.de

Abstract

Economic machining of brittle materials is enabled by ultra-precision grinding. A ductile material removal mechanism in precision grinding allows the generation of high surface qualities, low subsurface damage and tight tolerances.
For precision grinding of brittle materials, fine-grained grinding wheels are commonly used, as they reduce the maximum chip thickness and support ductile material removal. However, a disadvantage of fine-grained grinding wheels with soft bonds is their susceptiality to wear, which reduces efficiency and can lead to form errors. These disadvantages could be solved by coarse-grained grinding wheels with hard bonds. However, the application of coarse-grained grinding wheels is challenging due to the process design based on the critical and maximum chip thickness.
In this research, the applicability of a coarse-grained diamond grinding wheel with a grain size of D301 for ductile precision grinding of grooves in BK7 glass is investigated. For this purpose, the active grains on the circumference of the grinding wheel were identified and the expected material removal mechanism was calculated based on Malkin's maximum chip thickness equation. Cross grinding experiments with in-process force measurement were carried out to investigate the influence of feed rate and cutting speed on the material removal mechanism and surface generation. The evaluation of the prevailing material removal mechanism was assessed by surface texture and surface roughness, measured by white light interferometry.
Based on the results, it can be shown that ductile and ductile-brittle material removal occurs with the investigated grinding wheel. Feed rate and cutting speed have only limited influence on the material removal mechanism and the generated surface roughness. Furthermore, the force measurements show that not only individual grains are engaged during the grinding process, but rather clusters of grains.

Precision grinding, coarse-grained diamond grinding wheels, surface roughness, material removal mechanism

1. Introduction

Ultra-precision grinding enables the economical machining of optical and precision components made of brittle-hard materials. High surface qualities, low subsurface damage and tight tolerances can be achieved through ductile material removal [1, 2].

Fine-grained grinding wheels are generally used for precision grinding, as they reduce the maximum chip thickness and enable ductile material removal. However, fine-grained grinding wheels with soft bonds are susceptible to severe wear, which reduces the overall efficiency and productivity of the grinding process. Coarse-grained grinding wheels can be a solution to this problem, as they are less susceptible to wear due to their grain size and generally hard bond. However, the challenge when using coarse-grained grinding wheels is the process design based on the critical chip thickness [1,3].

In precision grinding of brittle-hard materials, the material removal mechanisms are crucial in generating the surface of the workpiece. According to Bifano, the material-dependent critical chip thickness $h_{cu,crit}$, as shown in (1), describes the maximum tolerable chip thickness, which in this context causes a ductile material removal mechanism and enables the machining of high surface qualities.

$$h_{cu,crit} = 0.15 * \left(\frac{E}{H}\right) * \left(\frac{K_c}{H}\right)^2 \quad (1)$$

E describes the modulus of elasticity, H the hardness and K_c the fracture toughness of the material; the factor 0.15 is a constant determined experimentally by Bifano et al. [4].

Exceeding the critical chip thickness leads to the formation of cracks and chipping as well as damage to the subsurface [4]. When designing grinding processes, the decisive parameter for calculating the transition from ductile to brittle machining is the maximum chip thickness $h_{cu,max}$, which has to fall below the critical chip thickness $h_{cu,crit}$ in order to machine ductilely [5]. The calculation of $h_{cu,max}$ according to Malkin requires the determination of the active cutting edge number C_{kin} and the grain shape factor r, as shown in (2) according to [5]. Other influencing variables are the feed rate v_w, the cutting speed v_c, the depth of cut a_e and the grinding wheel diameter d_s.

$$h_{cu,max} = \left(\frac{4 \cdot v_w}{v_c \cdot C_{kin} \cdot r} \sqrt{\frac{a_e}{d_s}}\right)^{1/2} \quad (2)$$

Based on Malkin's formula, the number of active cutting edges per surface and the grit size have an effect on the maximum chip thickness $h_{cu,max}$ and thus on the dominant material removal mechanism [5]. For this reason, fine-grained grinding wheels are generally used for precision grinding. They have a high grain density i.e. a high number of active cutting edges C_{kin} and small grain diameters which, according to (2), lead to a reduction in the maximum chip thickness and thus favour a ductile material removal mechanism. Furthermore, the stochastic distribution of the grains promote the applicability of the described calculation

formula. For example, with a high grain density, deviations of individual grains from the average grain form used in the formula are not significant. However, it is questionable whether this applies to coarse-grained diamond grinding wheels. Compared to fine-grained grinding wheels, coarse-grained grinding wheels have a low grain density and a stochastic distribution of the abrasive grains is only given to a limited extent. This has already been shown in earlier research work [6]. Based on the results shown in [6], a more detailed investigation of the application of a coarse-grained grinding wheel is to be carried out, focussing on the characteristics of the grinding wheel topography and detecting individual grain engagement in the force measurement. The aim is to gain a better understanding of the material removal mechanism.

2. Experimental setup, machining and analysing methods

In this research, plunge grinding experiments are carried out on BK7 glass with a coarse-grained diamond grinding wheel of grain size D301 with varying cutting speed v_c and feed rate v_w. The objective was to investigate to which extent ductile material removal can be realised with the coarse-grained diamond grinding wheel and whether individual grain impacts are recognisable in the force measurement in order to gain a better understanding of the process.

The grinding wheel applied is a galvanic bonded tool with blocky diamond grains, which was manufactured using reverse plating. According to the manufacturer, the envelope curve deviation is therefore less than 2 µm. The wheel has a radius of 40 mm and a spherical segment shape, which radius is also 40 mm.

To design the grinding experiments, the previously described formula for maximum chip thickness according to Malkin is applied. Therefore, it is necessary to determine grain density and active number of cutting edges respectively number of grains. This is carried out using a Keyence VHX-6000 digital microscope. The entire circumference of the grinding wheel is mapped. The area with a width of 2.2 mm of the grinding wheel that will later be in contact with the workpiece is then considered. This contact area was determined by the geometric contact conditions as well as previous work and is shown in Figure 1.

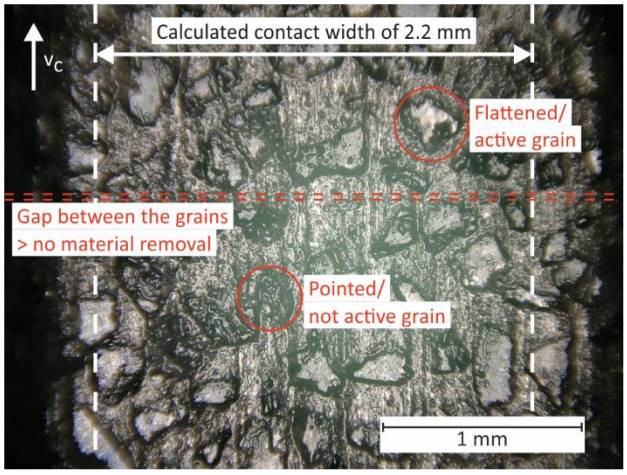

Figure 1. Exemplary digital microscopic measurement of the grinding wheel circumference with flattened and pointed grains

Within this area, the flattened grains are counted at four different positions in order to determine the grain density and the active grains. This is done under the assumption that flattened grains come into contact with the workpiece during the experiments and remove material. Pointed grains are assumed to be lower and thus non-active grains as they have not been flattened by the manufacturer's dressing process and are therefore not expected to come into contact with the workpiece. Based on the grinding wheel circumference it was furthermore be determined that the grains are grouped in a way that they overlap in a tangential direction and several grains will be engaged. However, there are also gaps between these grain clusters. No active grains can be found here and it can be assumed that material removal is not to be expected here. There are a total of four of these gaps on the grinding wheel circumference.

A grain density of 10.75 grains/mm^2 is determined. With the process parameters shown in Table 1, this results in a maximum chip thickness of 11.35 nm to 26.7 nm, depending on the selected parameter variation. As the specimens have a tip tilt of less then 4 µm for clamping reasons and in order to ensure full tool engagement after touching procedure, several grinding steps are carried out. At a feed rate v_w = 10 mm/min, three grinding steps with a depth of cut a_e of 2 µm are carried out first, followed by a grinding step with a_e = 3 µm. The last grinding step represents the actual experiment. The parameters are also listed in Table 1. In the experiments with a feed rate v_w of 15 mm/min, the specimens could be aligned more precisely. Therefore, only two grinding steps with an a_e of 2 µm are carried out first and then the final grinding step with a_e = 3 µm. The last grinding step again represents the actual experiment. The individual parameter combinations are each carried out three times in order to obtain a sufficient number of experiments for the evaluation and to be able to identify outliers. The kinematics of the grinding experiments are shown in Figure 2.

Table 1 Process parameters

Machine: Cranfield Precision TTG 350 Twin Turret Generator	
Material: N-BK7 glass	
Process: Plunge grinding	
Parameters:	
v_w = 10 mm/min	v_w = 15 mm/min
v_c = 30 ; 60 m/s	v_c = 30 ; 60 m/s
$a_{e,\ cut\ 1\text{-}3}$ = 2 µm	$a_{e,\ cut\ 1\text{-}2}$ = 2 µm
$a_{e,\ cut\ 4}$ = 3 µm	$a_{e,\ cut\ 3}$ = 3 µm
$h_{cu,max}$ = 20.01 ; 11.35 nm	$h_{cu,max}$ = 26.7 ; 15.07 nm
Grinding fluid: Emulsion	
Tools: Coarse-grained diamond grinding wheel, D301 (reverse plated)	

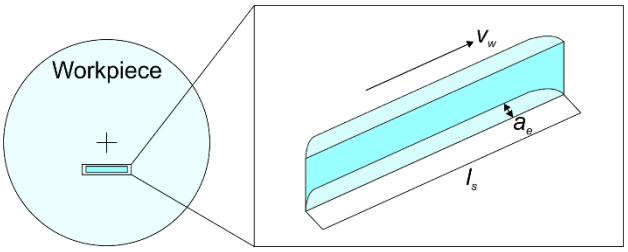

Figure 2. Kinematics of the plunge grinding experiments

Grinding experiments were performed on a Cranfield Precision TTG 350 Twin Turret Generator. The experimental setup is shown in Figure 3. A workpiece with a diameter of 50 mm and a thickness of 10 mm is mounted on a dynamometer type 9119AA1 from Kistler, which is clamped in the main spindle. The tool is located on the vertical grinding spindle. The process forces are measured at a measuring frequency of 50,000 Hz using inhouse software MesUSoft.

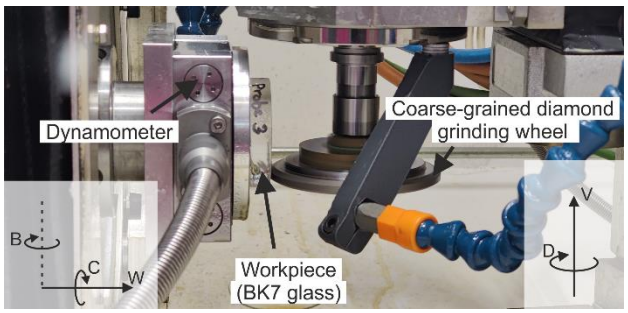

Figure 3. Experimental setup for plunge grinding experiments

The generated surface topography is measured using white light interferometry (WLI). A lens with 50x magnification and a measuring area of 0.34 mm x 0.34 mm is applied for topography characterisation. The generated depth of cut a_e is also measured using WLI. Here, a lens with 20x magnification and a measuring area of 0.84 mm x 0.84 mm as well as stitching is applied. Three measurements are carried out for each groove. The measurements are analysed using the commercial software Mountains 9.

3. Results and Discussion

As described in section 2, one machining step was omitted in the experimental sequence with v_w = 15 mm/min, as the specimens were already well aligned. The total depth of cut was determined to ensure that the depth of cut was achieved and that further evaluation of the experiments was reasonable. The depth of cut should be 9 µm at v_w = 10 mm/min and 7 µm at v_w = 15 mm/min. The results of the measurements are shown in Figure 4. The bars represent the mean value of all measurements and the error bars represent the minimum and maximum measured depth of cut. It can be seen that the intended depth of cut could be obtained with deviations. These deviations are shown by the error bars, which represent the maximum and minimum measured depth of cut of the grooves. The indicated deviation can be explained by two effects. Foremost, the specimens have a tip tilt due to the clamping technique, which can affect the actual depth of cut. Furthermore, a touching procedure is carried out before machining each groove to determine the surface of the samples. As this is done manually, there may also be slight deviations that affect the overall depth of cut. Except with the parameter combination with v_c = 30 m/s and v_w = 10 mm/min. However, the depth of cut of the final grinding step could also be realised in all experiments. It can therefore be assumed that the last grinding step of experiments were carried out with the intended set of parameters.

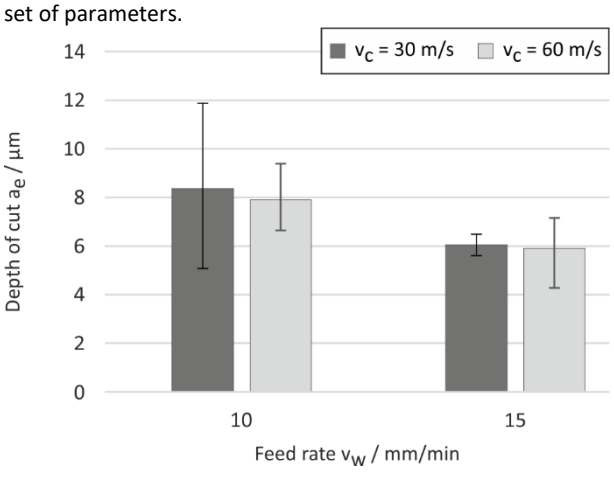

Figure 4. Generated depth of cut a_e

The generated surfaces are measured as described using WLI. The tip-tilt of the measurements is removed by alignment and a cut-off wavelength of 80 µm is used to separate waviness from roughness.

The mean arithmetic height of the generated surfaces and their deviation is shown in Figure 5. Roughness Sa between 55 nm and 88 nm generated. The lowest roughness Sa occured at v_w = 15 mm/min and v_c = 60 m/s. However, there is no recognisable significant influence of the feed rate and cutting speed on the generated surfaces. The measured surface roughness is similar and the areas of deviation partially overlap. This could be due to brittle breakout during machining, as shown in Figure 5. This is particularly noticeable at v_c = 60 m/s and v_w = 15 mm/min. Although the lowest mean arithmetic height Sa is measured here, the highest deviation is present once again.

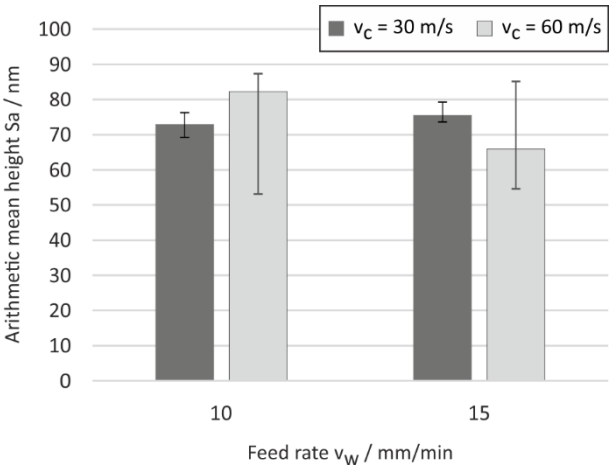

Figure 5. Measured arithmetic mean height Sa

Based on the qualitative analysis of the generated surfaces, which is shown exemplarily in Figure 6, it can be seen that the dominant material removal mechanism was ductile or ductile-brittle. There is only isolated brittle breakout visible. With a cutting speed v_c of 30 m/s, almost entirely ductile material removal was realised. At a cutting speed of 60 m/s, a ductile-brittle material removal mechanism occurs. There are large areas that indicate a ductile material removal and also smaller areas with brittle breakout and irregular surface morphology, which indicate a rather brittle material removal mechanism. This also explains the described deviation of the determined arithmetic mean height Sa.

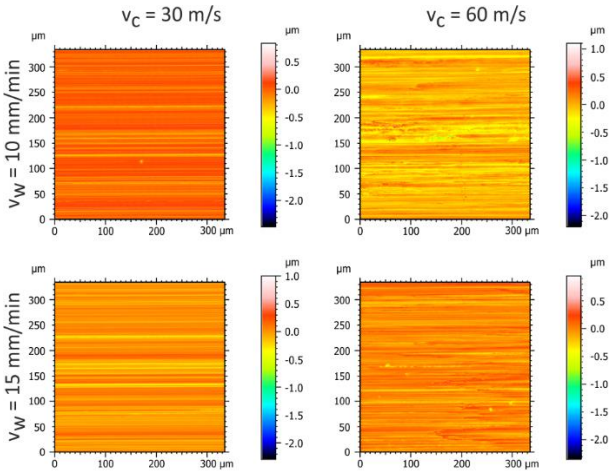

Figure 6. Qualitative comparison of the generated surfaces

Figure 7 shows the mean normal forces F_N that occurred during the experiments. The deviation is not shown in this figure, because dynamic effects with high deviations from the mean value occurred in some cases, which do not allow a reasonable representation. Figure 6 shows a clear influence of the cutting speed vc on the normal force F_N. With a higher cutting speed, significantly lower normal forces occur. This can be explained by the decrease in the maximum chip thickness, which is given by a higher cutting speed. The influence of feed rate, on the other hand, is marginal and does therefore not allow any clear conclusions to be drawn.

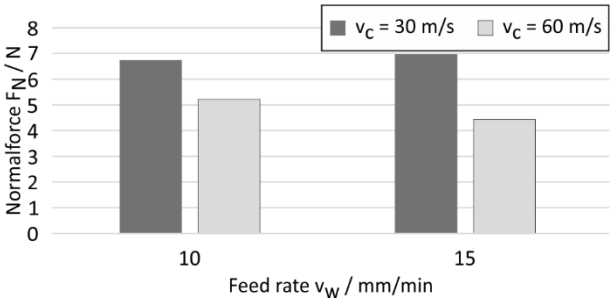

Figure 7. Mean normal force F_N of the grinding experiments

Figure 8 shows an example of the force measurement of four grinding wheel rotations in an experiment with a cutting speed v_c of 30 m/s and a feed rate v_w of 15 mm/min. It can be seen that the normal force is almost identical for all four grinding wheel rotations and it can therefore be assumed that the contact conditions remain the same. The figure shows furthermore the dynamic effects not previously shown in Figure 6, which in some cases lead to very high normal forces. This can be attributed to individual grains that protrude slightly further from the bond and therefore remove more material. It is also noticeable that the normal force F_N falls back to 0 N four times, which indicates an interrupted cut. The number of these interruptions corresponds with the number of gaps between the grain clusters of the grinding wheel, which were described in section 2. Furthermore, the individual high peaks indicate single-grain interactions, but these do not correspond to the number of single grains present in the grain clusters. Instead, several individual grains appear to overlap, so that only isolated single-grain interactions can be recognised.

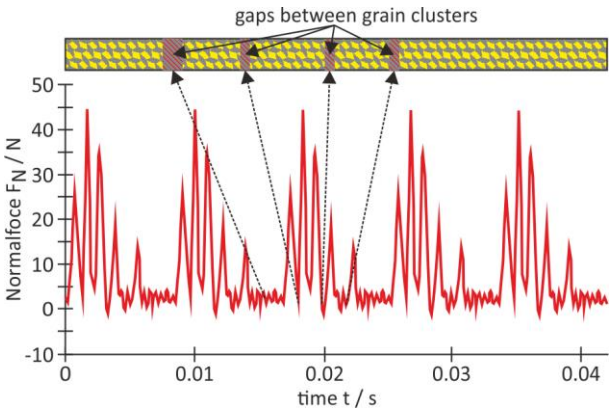

Figure 8. Force measurement of four grinding wheel rotations in an experiment with a cutting speed v_c of 30 m/s and a feed rate v_w of 15 mm/min

4. Summary and conclusions

With a coarse-grained diamond grinding wheel relatively low roughness below 100 nm can be generated in BK7 and mainly ductile and ductile-brittle material removal is present. However, the generated surface roughness is too high for ultra-precision applications and therefore further finishing process steps are required.

A significant influence of the cutting speed v_c and the feed rate on the generated surface roughness could not be determined.

When analysing the normal forces F_N, no detectable influence of the feed rate v_w on the forces and their characteristics could be determined either. However, an influence of the cutting speed v_c on the normal forces is detectable and manifests itself in decreasing normal forces with increasing cutting speed. This can be explained by the decreasing chip thickness with increasing cutting speed or rotational speed of the grinding wheel.

A more detailed examination of the force measurements and the normal forces occurring for each of four grinding wheel rotations shows that the force is almost identical for each rotation. Furthermore, there are points in the force curves where the normal force drops to 0 N. The number of these points coincides with the previously determined gaps between the grain clusters on the grinding wheel circumference. Furthermore, only isolated single grain interactions can be detected in the force, which do not correspond to the expected number of engagements. It is therefore assumed that several individual grain engagements are superimposed and that a single grain analysis is not sufficient to make further conclusions about the material removal mechanism. Rather, another approach must be found to assign the occurring forces to the material removal mechanism and the contact conditions between the grinding wheel and the workpiece.

5. Future work

Current work is focussing on the analysis of additional coarse-grained grinding wheels up to a grain size of D1001. The aim here is no longer to analyse individual grains but to measure the grinding wheel circumference in order to determine the grinding wheel topography. Using the height information obtained and high precision force measurements, the objective is to determine the load stresses in the contact zone.

Acknowledgements

This work is supported by the German Research Foundation (DFG) under Grant No. HE 3276/10-1, Project No. 435367659.

References

[1] Brinksmeier E, Mutlugünes Y, Klocke F, Aurich J C, Shore P, Ohmori H 2010 Ultra-Precision Grinding CIRP Ann. 59 P 652-671

[2] Wang, J; Li, Y; Han, J; Xu, Q; Guo, Y Evaluating subsurface damage in optical glasses In Journal of the European Optical Society – Rapid Publications, 2011, 6/11001; S1-16

[3] Brinksmeier E, Riemer O, Rickens K, Berger D 2016 Application potential of coarse-grained diamond grinding wheels for precision grinding of optical materials. Prod. Eng. 10 P 563–573

[4] Bifano T G, Dow T A, Scattergood R O 1991 Ductile-regime grinding: a new technology for machining brittle materials. Trans. o. t. ASME, Journal of Engineering for Industry 113 P 184–189

[5] Malkin S 1989 Grinding Technology - Theory and Application of Machining with Abrasives, Ellis Horwood Ltd

[6] Adam, B., Riemer, O., Rickens, K., Heinzel, C. 2023. Precision grinding of BK7 glass with coarse-grained diamond grinding wheels. euspen – ICE 2023, Copenhagen, DK, P 501-502.